Terahertz spectroscopy coupled with multivariate analysis for non-invasively evaluating flavonoids extracts from waste orange peels

Chao-Hui Feng[a, b*], Chiko Otani[b, c*], Yuichi Ogawa[d]

[a] School of Regional Innovation and Social Design Engineering, Faculty of Engineering, Kitami Institute of Technology, 165 Koen-cho, Kitami, Hokkaido, 090-8507, Japan.

[b] RIKEN Centre for Advanced Photonics, RIKEN, 519-1399 Aramaki-Aoba, Aoba-ku, Sendai, 980-0845, Japan

[c] Department of Physics, Tohoku University, 6-3 Aramaki-Aoba, Aoba-ku, Sendai, Miyagi 980-0845, Japan

[d] Division of Environmental Science & Technology, Graduate School of Agriculture, Kyoto University, Kitashirakawa-Oiwakecho, Sakyo-ku, Kyoto, 606-8502, Japan

[*] Corresponding author. School of Regional Innovation and Social Design Engineering, Faculty of Engineering, Kitami Institute of Technology, 165 Koen-cho, Kitami, Hokkaido, 090-8507, Japan; RIKEN Centre for Advanced Photonics, RIKEN, 519-1399 Aramaki-Aoba, Aoba-ku, Sendai, 980-0845, Japan. E-mail: feng.chaohui@mail.kitami-it.ac.jp

[*] Corresponding author. RIKEN Centre for Advanced Photonics, RIKEN, 519-1399 Aramaki-Aoba, Aoba-ku, Sendai, 980-0845, Japan; Department of Physics, Tohoku University, 6-3 Aramaki-Aoba, Aoba-ku, Sendai, Miyagi 980-0845, Japan E-mail: otani@riken.jp

Abstract

Fourier transform far-infrared (FT-FIR) was exploited to evaluate the flavonoids content of orange extracts using Soxhlet extraction. The absorbance fingerprint spectra of hesperidin and naringin were identified in the range of 0.5 - 7 THz. Pre-treatments such as normalization, standard normal variate (SNV), multiplicative scatter correction (MSC), 1^{st} and 2^{nd} derivation were employed to enhance the robustness of the model performance. Partial least square regression model performed well to explain the relationship between THz spectra and concentrations of hesperidin and naringin, with the determination coefficients of prediction up to 0.99 (pre-treated by 1^{st} deviation) for hesperidin and 0.97 for naringin, respectively. This study addressed the detection of hesperidin and naringin by using terahertz spectroscopy, which could potentially simplify the procedures to detect the flavonoids of orange extracts from waste orange peels.

Keywords: terahertz, orange extracts, hesperidin, naringin, chemometrics

1. Introduction

Terahertz falls in the frequency range of 0.1-10 THz (1 THz = 10^{12} Hz) and the photon energy (4 meV for 1 THz) is much lower than that of X-ray photons (100 eV – 100 keV), the radiation of which is much safer for operator in comparison of X-ray based equipment. Moreover, it is an exceptional tool to investigate numerous materials whose molecular or crystal structures are stabilized by the weak interactions because the THz frequency associated with the low-frequency vibration and the vibration modes of weak interactions (Ueno and Ajito, 2008). As an emerging and cutting-edge technology,

terahertz spectroscopy (THz) has been intensively employed to detect biology threats and defects (Liu et al., 2007), residue detection (Suzuki et al., 2011; Qin et al., 2017), transgenic food (Liu and Li, 2014; Liu et al., 2016), foreign body detection (Ok et al., 2014; Wang et al., 2019), dynamical changes in seeds (Li et al., 2018; Nakajima et al., 2019) and adulteration (Liu 2016). However, the application of terahertz spectroscopy in foodstuffs is still at infant stage in comparison with the sophisticated and prevalent spectroscopic and imaging techniques like hyperspectral imaging (Cheng et al., 2016; Feng et al., 2020a), Raman spectroscopy (Karacaglar et al., 2019), and NIR images (Huang et al., 2017). This is because water is strong THz wave absorber, which is the major hurdle for comprehensive application of THz in the food industry (Gowen et al., 2012, Feng and Otani, 2020). Hitherto, little relevant study on identifying the feature spectra of flavonoids and the flavonoids extracts from waste orange peels in the THz range.

Citrus fruit peels contain a large amount of biologically active compounds such as phenolic acids and flavonoids could prevent various diseases (Toledo-Guillén et al., 2010; Gómez-Mejía et al., 2019;). In Japan, approximately 400 thousand tons of fruits juice is annually consumed and around 2,000 ton of oranges are treated each year in the JA (Japan Agricultural Cooperative) Foods Factory in Shizuoka prefecture, which generates 1,000 ton of waste (Ishiwata et al., 2013). The amount of orange production in Shizuoka prefecture is just about 11% among Japan, and approximately 10 times of wasted could be produced. It is highly costly to deal with the waste to obey the Food Recycling Law in Japan (Anon. 2006; 2007). The waste orange peels are either discarded directly to landfills as

fertilizer or used as an animal feed or sold as dried orange peels to China as one of the ingredients of Chinese herbal medicine (Ishiwata et al., 2013). Flavonoids in orange peel possess properties of antioxidant, anti-cancer, antimicrobial (Sawalha et al., 2009), and was reported to potentially inhibit coronavirus (Bellavite and Donzelli, 2020; Jo et al., 2020; Li et al., 2020). If they can be extracted from waste orange peels and fully utilised, it can not only maximise the reuse and reduce environmental problem, but also exploit the value-added by-products and cut down industrial economical costs (Feng et al., 2020b). Comprehensive researches have been studied to optimise the extraction processing of flavonoids from citrus peels by using high-pressure processing (Ancos et al., 2020), subcritical water (Kim and Lim, 2020), ultrasound (Wang and Wang, 2019), and by different organic solvents using Soxhlet extraction (Park, et al., 2014; Feng et al., 2020b). Naringin and hesperidin are the most abundant flavonoids in orange peel (Sawalha et al., 2009) and they are commonly identified by high-performance liquid chromatographic (HPLC) system (Uchiyama et al., 2008; Belboukhari et al., 2009). As the retention times (RT) for naringin and hesperidin were detected approximately 5.66 min and 5.91 min via ultra-high performance liquid chromatography high-resolution mass spectrometry (UHPLC-HRMS/MS) (Feng et al., 2020b), whose RT is very close due to the similar molecule structure, there is a need to exploit the easy method to distinguish those chemical components. Ueno and Ajito (2008) have pointed out that THz is an ideal and effective method for identifying intermolecular interactions in chemical compounds and enable to detect weak inter- and intramolecular vibrational modes. In addition, if the information for flavonoids contain in

orange peel can directly obtain via THz, it will save a lot of time and free from the tedious and complicated extracting procedures. Since scarce information is available in literature on identifying the naringin and hesperidin in the terahertz range, the determined fingerprint of those spectra could update the terahertz database and so potentially be an alternative method to non-invasively detect the flavonoids in the dried orange peels or orange extracts.

The primary objective of this work is thus to qualitatively identify the naringin and hesperidin fingerprint spectra in the terahertz range. Following this, the quantitative models relating the terahertz spectra data to the reference concentration of hesperidin and naringin are established via partial least squares regression (PLSR). Subsequently, the THz spectra comparison between standard pure hesperidin, naringin, orange powder, and flavonoids extracts from waste orange peels are conducted.

2. Materials and methods

2.1 Soxhlet extraction

Based on the previous optimal sample preparation method (Feng et al., 2020b), the peels of Valencia sweet orange (*Citrus sinensis*) were dried at oven (45 ^{o}C) for 7 days and approximately 40.36 ± 0.37g finely blade-milled orange power was put into a cartridge (sealed with cotton) for Soxhlet extraction using 250 ml of methanol or ethanol. The concentration of solvent (i. e. methanol and ethanol) were 80% (80 : 20, v/v) and 100%, respectively. A rotary evaporator was used to separate the extract from solvent and the extract was put in a flow hood overnight to let the solvent evaporate completely and

so to obtain the crude extracts (Feng et al., 2020b). Afterwards, those crude extracts were washed by distilled water as twice as their weights, filtered and dried stored in a desiccator (to obtain precipitate extracts). The efficiencies of crude extract (E_c) and precipitation (E_p) were determined using the following equation:

$$E_c = \frac{W_c}{W_o} \times 100\% \quad (1)$$

$$E_p = \frac{W_p}{W_o} \times 100\% \quad (2)$$

Where W_c, W_p and W_o were the weight of the crude, precipitated extract and the orange powder, respectively. All the experiments were carried out in triplicates.

2.2 Tablets preparation

Orange powder was dried 9 days (45 ^oC) before making the tablets to eliminate the water content whilst for flavonoids extracts, they were vacuum dried at 20 ^oC for 9 days before making tablets. The milled standard hesperidin powder (Tokyo Chemical Industry Co. LTD, Tokyo, Japan), milled standard naringin powder (Sigma-Aldrich, Saint Louis, USA), milled orange powder and milled flavonoids extracts were screened by a sieve with a size of 45 μm. Polyethylene (P. E.; Shamrock Technologies, Newark, New Jersey, USA) was dried at 80 ^oC overnight and screened by a sieve with a size of 212 μm. The total volume for making the tablet was 0.20 ± 0.05g. Standard hesperidin and naringin matrices tablets were made in different concentrations, being mixed with P. E., ranging from 5% - 70% (wt.). The tablet concentrations for orange powder was 50% (wt.). A hand press (SSP-10A, Shimadzu,

Japan) was used to compress the finely mixed powder to tablets under the load of 8 N. The average diameter and thickness of pellets were 13.11 ± 0.11 mm and 0.64 ± 0.01 mm, respectively.

2.3 Fourier transform far-infrared (FT-FIR) spectrometer

THz spectra were obtained by a FT-FIR (JASCO, FARIS) coupled with a superconducting bolometer (QMC, QNbB/PTC). A high-pressure mercury lamp was used as the light source, and a wire-grid beam splitter was used for the measurement with the resolution of 0.24 THz. A total of 200 scans were accumulated in 3 min to obtain a single spectrum. The samples were horizontally placed on an optical aperture with a diameter of 5.89 ± 0.02 mm in the sample chamber of the spectrometer. The sample chamber was purged by a continuous flow of nitrogen gas with rate of 30L/min, to reduce the absorption of water vapor. Sample was left in the chamber for 2 min before measurement. The frequency dependence of absorbance (A) was calculated according to the following equation:

$$A = - \log_{10} \left(\frac{I_a(\omega)}{I_b(\omega)}\right) \quad (3)$$

where $I_a(\omega)$ and $I_b(\omega)$ were the power spectra of the sample and reference, respectively. The corrected absorbance of the sample tablets ($A_{corrected}$) mixed with P. E. can thus be obtained as follows:

$$A_{corrected} = A_1 - (1 - m) \times A_2 \quad (4)$$

where A_1 is the measured absorbance of sample tables and A_2 is the absorbance of 100% pure P. E., respectively. m is the concentration of the matrix's tablets. All the measurements were conducted at

least in triplicate at room temperature (21-23 ^{o}C). The experiments were repeated in the Kyoto University as well, to test its repeatability.

2.4 Regression model development and performance evaluation

Several spectra pre-treatments, including multiplicative scatter correction (MSC), normalisation, standard normal variate (SNV), first and second derivative, were carried out to improve the performance of the model before the multivariate analysis using Unscrambler software (version 11.0, CAMO Software Inc., Trondheim, Norway). One third of the total measured samples were selected for the prediction group and the rest two thirds was utilised as the calibration group.

A PLSR model was used to establish the calibration models in the full absorbance spectral range of 0.5 - 7 THz for data obtained from FT-FIR spectrometer. The PLSR model can be obtained by using regression coefficients and weight values for corresponding frequencies:

$$\text{PLSR} = \sum_{i=1}^{m} F_i R_i + C \quad (5)$$

where F_i and R_i are the i^{th} frequency and the corresponding regression coefficient obtained from the PLSR model. C stands for the constant of the PLSR model.

The evaluation of model performance is to ensure the predictive ability and model robustness. The determination coefficients of prediction (R_p^2), calibration (R_c^2), and cross validation (R_{cv}^2); the root mean square errors of prediction (RMSEP), calibration (RMSEC), and full cross validation (RMSECV) were used for estimating the predictive capabilities of the model. It is commonly believed that a good

PLSR model possesses a high R^2 with a low RMSE along with a small absolute difference between RMSEC and RMSECV.

3. Results and discussion

3.1 Spectral characteristics overview for standard hesperidin and naringin matrices tablets measured with FT-FIR

Hesperidin, which is rich in the citrus fruits such as lemon and sweet orange, is effectively against liver cancer, breast cancer (Lee et al., 2010), lung cancer (Al-Jasabi and Abdullah, 2013) and so on. It can scavenge and inactivate the alkyl peroxyl radicals and superoxide radicals those are harmful in the organism (Chen et al., 2010). Besides, the injuries due to free radicals can be avoided due to its high chemical reactivity, such as inducing antioxidant enzymes, metal ions chelating, reducing in α-tocopherol radicals, inhibiting oxidases, and increasing in antioxidant effects of low molecular antioxidants (Chen et al., 2010; Roohbakhsh et al., 2015). Flavonoids have been comprehensively exploited to skincare products due to its antioxidant, anti-ageing, anti-inflammatory, antimicrobial, and anticancer properties (Feng et al., 2020b). Currently, flavonoids are reported to potentially inhibit coronavirus (Jo et al., 2020, Li et al., 2020). Latest literature also shows that flavonoids (e. g. hesperidin and rutin) possess a better binding affinity to main protease of COVID-19 than nelfinavir and so could be regarded as the starting point for therapeutics against COVID-19 (Adem et al., 2020). Likewise, hesperidin was reported to be the most suitable substance to bind to the “spike” of SARS-CoV-2 after

testing 1066 natural substances with potential antiviral effect as well as 78 antiviral drugs (Wu et al. 2020). As the invasion of SARS-CoV-2 is mediated by binding its spike glycoprotein with its receptor (ACE2) on the host cell membranes, hesperidin will interrupt the binding of SARS-CoV-2 with ACE2 via superimposing the ACE2 and forming the receptor binding domain complex on the hesperidin (Bellavite and Donzelli, 2020). Another hypothetical site is a lower energy is requested for binding hesperidin with SARS-CoV-2 (compared with 1500 screened potential molecules), which prevents this virus to bind with the host cell (Chen et al., 2020).

Figure 1 (a) and (b) illustrate the absorbance spectra measured with different concentrations of hesperidin and naringin using FT-FIR, respectively. The absorption peaks of hesperidin were obtained at 1.53, 1.85, 2.46, 3.36, 4.51, 5.35, 6.51, and 7.55, respectively. The absorbance spectra higher than 2.5 is unshown because absorbance higher than 2.5 is meaningless (i. e. no significant spectral component). Stanisic et al. (2020) utilised the Fourier Transform-Infrared spectroscopy to detect the absorption bands of hesperidin-copper complex, where the peaks were observed at 38.88 THz (1297 cm^{-1}), 38.22 THz (1275 cm^{-1}), 37.23 THz (1242 cm^{-1}), 36.15 THz (1206 cm^{-1}), 35.50 THz (1184 cm^{-1}), 34.60 THz (1154 cm^{-1}), 33.94 THz (1132 cm^{-1}), 32.83 THz (1095 cm^{-1}), 31.60 THz (1054 cm^{-1}), 31.09 THz (1037 cm^{-1}), and 30.25 THz (1009 cm^{-1}), respectively.

As a glycosylated flavone, naringin is commonly used as a flavouring in bakery products, beverages and perfumery. It possesses a bitter taste, which could potentially replace caffeine or quinine for tonic beverages (Feng et al., 2020b). Naringin is capable to prevent citrus from lipid peroxidation (Maleki

et al., 2019). As naringin presented the lowest binding energy (-9.8 Kcal/mol) with the spike protein of the COVID-19, this shows the highest binding affinity with the spike protein of SARS-CoV-2 and could potentially use for developing COVID-19 related therapies (Jain et al., 2020). As depicted in Figure 1 (b), the absorption peaks of naringin were observed at 0.78, 1.50, 2.29, 3.79, 5.15, 6.48, and 8.36 THz, respectively. The standard tablets of hesperidin and naringin were made at Kyoto University and obtained the same spectra peak, which indicates the experimental results are trustful and reproduceable.

Hesperidin and naringin can be clearly distinguished using THz spectroscopy (Fig. 2). The perceptible absorption peaks at 3.76, 4.40, and 5.18 THz can be observed from fingerprint spectra of naringin whilst those peaks cannot be detected from the hesperidin THz spectrum. Likewise, the noticeable absorption peaks at 3.36, 4.51, 5.35, and 8.19 THz can be obtained from fingerprint spectra of hesperidin whereas they are indiscernible from the naringin THz spectrum. As aforementioned, the retention times (RT) for naringin and hesperidin were very close (Feng et al., 2020b). This novel technology could simplify the complex and time-consuming processing that occurred at HPLC processing and could be more practically and efficiently appliable to pharmaceutical industry. Last but not least, the identified hesperidin and naringin THz spectra peaks could update THz database.

3.2 Spectral characteristics overview for tablets made from orange peel powder and orange extracts measured with FT-FIR

Average THz spectra of tablets made from dried orange powder, standard hesperidin and naringin were shown in Figure 3 (a). The THz spectra of orange powder do not possess distinguished fingerprint peak compared to that of standard hesperidin and naringin. Two possibilities: (1) Hesperidin and naringin in the orange powder are both non-crystalline and/or (2) the amount of hesperidin and naringin is too small to see their specific spectral features. Further investigation shows that the extracts from the orange peels possessed a similar THz fingerprint of hesperidin regardless of the extraction solvents [Fig. 3 (b) & (c)]. The vibration between molecules in orange peels may attribute to this phenomenon. For example, amino acids have many peaks, but peptides and proteins have gradually obscured peaks. Compared to the conventional detection method such as HPLC, this method is novel and more advantageous as it is easy, rapid and robust, being free from the complex preparation and detection procedures. As the efficiency of precipitate extract using 100% concentration of solvents is higher than that of 80% (Table 1), the tablets that made from precipitate extract using 100% concentration of solvents contain a higher concentration. For example, the concentrations of making the tablets using 100% and 80% methanol were 25.02% and 8.87%, respectively. The concentrations for making the tablets using 100% and 80% ethanol were 37.43% and 6.36%, respectively. As a result, the absorbances of tablets made using 100% extraction solvents [Fig. 3 (b)] were higher than that using 80% extraction solvents [Fig. 3 (c)].

3.3 Calibration models at selected frequencies

As a useful approach to mine the spectral data, chemometric analysis has been comprehensively applied to Raman spectroscopy (Nunes et al., 2019), near infrared spectroscopy (García-Martín 2015; García-Martín, et al. 2019a, 2019b), and hyperspectral imaging (Cheng and Sun, 2015; Cheng et al., 2017; Feng et al., 2018), to explain the relationship between the measured parameters and spectra data. Partial least square regression (PLSR), one of the most common chemometric analyses, has been employed to analyse data with collinear variables in the independent (X) and dependent variables (Y) (Feng and Makino, 2020). The relationship between THz spectra and corresponding tablets concentration were developed by the PLSR model. The noise and redundancy data were removed in order to improve the performance of the model. To this end, the ranges of 0.5 - 7 THz were selected for hesperidin and naringin samples measured by FT-FIR, respectively. For hesperidin sample, the model using the data acquired from FT-FIR overall could achieve a high R_c^2 (range from 0.91 - 0.99) and R_p^2 (range from 0.89 - 0.99) (Table 2). For naringin sample, R_c^2 and R_p^2 can reach up to 0.99 and 0.97, respectively. As mentioned by Girolamo et al., (2009), R^2 value that falls in the range of 0.66 to 0.81 indicates approximate quantitative prediction ability of the model whilst the R^2 value between 0.82 and 0.90 implies a good prediction. Excellent prediction can be obtained if the R^2 value is over 0.91 (Girolamo et al., 2009). In this case, the model performed well when using the data obtained from FT-FIR for both hesperidin and naringin samples. For the naringin sample, the model performances of data with different pre-treatments were not greatly improved compared with the raw data. With regard to hesperidin sample, the R_p^2 value of model derived from 1st Deviation improved from 0.98 to 0.99,

with the reduction of RMSEP from 3.52% to 2.97%. The improved performance may be due to the removal of the background noise and baseline drift caused by 1st deviation (Shen et al., 2012). MSC is a transformation method, which could compensate for additive and multiplicative effects (Helland et al., 1995) whilst SNV is usually employed to remove variability in the reflectance spectra caused by light scattering (Jia et al., 2017). Comparably, the imidacloprid concentration within the rice powder was detected using THz-TDS in the range of 0.3 and 1.7 THz (Chen et al., 2015). The optimal frequency range with different number of intervals has been selected by interval partial least squares (iPLS) and the highest R^2 can reach up to 0.9963 with RMSECV of 0.35.

The innovative points for current study are shown as follows:

1. The fingerprint THz spectra of hesperidin and naringin were for the first time identified by using FT-FIR, which could fill the absent THz database and providing the useful information for the deeper investigation.
2. The relationship between concentration of hesperidin/naringin and THz absorbance spectra were for the first time established by using partial least square regression model, with the high coefficients of determination for calibration (up to 0.99) and prediction groups (up to 0.99) and the low RMSEC (lower to 0.70%) and RMSEP (lower to 2.97%).
3. The extracts from waste orange peels by using Soxhlet Extraction were novelty detected by terahertz spectroscopy, which potentially simplifies the complex and time-consuming conventional analysis (such as HPLC).

4. Conclusions

The feature spectra of hesperidin and naringin were successfully detected by FT-FIR, which updates the THz database for hesperidin and naringin. Multivariate regression method like PLSR has been employed for elucidating the relationship between the concentration of the hesperidin/naringin and THz spectra. The determination coefficient of prediction model for hesperidin concentration devised by THz spectra (THz selected range: 0.5 - 7 THz) pre-treated with 1st derivation was 0.99 with the RMSEP of 2.97. As for naringin, PLSR model with raw data achieved a higher R_p^2 result (R_p^2 = 0.97) with a lower RMSEP (4.48) compared with other pretreatments. The orange extracts were for the first time detected by terahertz spectroscopy and identified to contain hesperidin in an easier way. Terahertz spectroscopy, as an emerging and non-invasive approach, can rapidly evaluate the hesperidin content directly from the orange extracts, demonstrating its powerful and fast analysis in online and off-line inspections.

Acknowledgements

Chao-Hui Feng wishes to acknowledge the financial support of her research work under JSPS Grant-in-Aid for Early-Career Scientists (20K15477), Leading Initiative for Excellent Young Researchers (LEADER) from Ministry of Education, Culture, Sports, Science and Technology (MEXT) (2020L0277), FY 2021 President's Discretionary Grants, funded by Kitami Institute of Technology, Special Postdoctoral Researcher Program, and Exploratory "Collaboration Seed" fund at Riken. The

authors would also like to thank Hiromichi Hoshina from RIKEN Centre for Advanced Photonics for the experimental assistance and borrowing FT-FIR and the anonymous reviewers for their constructive comments.

Reference

Adem, S., Eyupoglu, V., Sarfraz, I., Rasul, A. & Ali, M. (2020). Identification of potent COVID-19 main protease (Mpro) inhibitors from natural polyphenols: An in silico strategy unveils a hope against CORONA, *Preprints*, 2020030333.

Al-Jasabi, S. & Abdullah, M. (2013). The role of antioxidant hesperidin in the attenuation of lung cancer caused by benzo[a]pyrene in Balb/c mice. *World Applied Sciences Journal,* 22: 1106–1110.

Ancos, B. D., Rodrigo, M. J., Sánchez-Moreno, C., Cano, M. P. & Zacarías, L. (2020). Effect of high-pressure processing applied as pretreatment on carotenoids, flavonoids and vitamin C in juice of the sweet oranges 'Navel' and the red-fleshed 'Cara Cara'. *Food Research International,* 132, 109105.

Anonymous (2006). Law for promotion of recycling and related activities for the treatment of cyclical food resources (Food Waste Recycling Law). Available at http://www.env.go.jp/en/laws/recycle/10.pdf

Anonymous (2007). Japanese cabinet approves bill to amend food recycling law. Available at https://www.japanfs.org/en/news/archives/news_id026664.html

Belboukhari, N., Cheriti, A., Roussel, C. & Vanthuyne, N. (2010). Chiral separation of hesperidin and naringin and its analysis in a butanol extract of *Launeae arborescens*. *Natural Product Research,* 24, 669–681.

Bellavite, P. & Donzelli, A. (2020). Hesperidin and SARS-CoV-2: new light on the healthy function of citrus fruits. *Antioxidants*, 9, 742.

Chen, M. C., Ye, Y. Y., Ji, G. & Liu, J. W. (2010). Hesperidin upregulates heme oxygenase-1 to attenuate hydrogen peroxide-induced cell damage in hepatic L02 cells. *Journal of Agricultural and Food Chemistry*, 58, 3330–3335.

Chen, Z. W., Zhang, Z. Y., Zhu, R. H., Xiang, Y. H., Yang, Y. P. & Harrington, P. B. (2015). Application of terahertz time-domain spectroscopy combined with chemometrics to quantitative analysis of imidacloprid in rice samples. *Journal of Quantitative Spectroscopy & Radiative Transfer*, 167, 1–9.

Chen, Y. W., Yiu, C. B. & Wong, K. Y. (2020). Prediction of the SARS-CoV-2 (2019-nCoV) 3C-like protease (3CL(pro) structure: Virtual Screening reveals velpatasvir, ledipasvir, and other drug repurposing candidates. *F1000Research*, 9, 1–17.

Cheng, J. H., and Sun, D.-W. (2015). Rapid and non-invasive detection of fish microbial spoilage by visible and near infrared hyperspectral imaging and multivariate analysis. *LWT- Food Science and Technology*, 62, 1060–1068.

Cheng, W. W., Sun, D.-W. & Cheng, J. H. (2016). Pork biogenic amine index (BAI) determination based on chemometric analysis of hyperspectral imaging data. *LWT- Food Science and Technology*, 73, 13–19.

Cheng, L. N., Sun, D.-W., Zhu, Z. W., and Zhang, Z. H. (2017). Effects of high pressure freezing (HPF) on denaturation of natural actomyosin extracted from prawn (Metapenaeus ensis). *Food Chemistry*, 229, 252–259.

Feng, C. H., Makino, Y., Yoshimura, M. & Rodríguez-Pulido, F. J. (2018). Recent advances for rapid detection of quality and safety of fish by hyperspectral imaging analysis. In Nollet, L. M. L. (Ed.), *Hyperspectral Imaging Analysis and Applications for Food Quality* (Chapter 12). CRC Press, Taylor & Francis LLC. ISBN:978-1-138-63079-6

Feng, C. H. & Makino, Y. (2020) Colour analysis in sausages stuffed in modified casings with different storage days using hyperspectral imaging – A feasibility study. Food Control 2020, 111, 107047.

Feng, C. H. Makino, Y. & García-Martín, J. F. (2020a). Hyperspectral imaging coupled with multivariate analysis and image processing for detection and visualisation of colour in cooked sausages stuffed with different modified casings. *Foods*, 9, 1089.

Feng, C. H., García-Martín, J. F., Lavado, M. B., López-Barrera, M. C. & Álvarez-Mateos, P. (2020b). Evaluation of different solvents on flavonoids extraction efficiency from sweet oranges and ripe and immature Seville oranges. *International Journal of Food Science and Technology*, 55, 3123–3134.

Feng. C. H. & Otani, C. (2020). Terahertz spectroscopy technology as an innovative technique for food: Current state-of-the-Art research advances. *Critical Reviews in Food Science and Nutrition,* in press.

García-Martín, J. F. (2015). Optical path length and wavelength selection using Vis/NIR spectroscopy for olive oil's free acidity determination. *International Journal of Food Science and Technology,* 50, 1461–1467.

García-Martín, J. F., Alés-Álvarez, F. J., Carmen López-Barrerz, M. D., Martín-Domínguez, I. and Álvarez-Mateos, P. (2019a). Cetane number prediction of waste cooking oil-derived biodiesel prior to transesterification reaction using near infrared spectroscopy. *Fuel,* 240, 10–15.

García-Martín, J. F., Carmen López-Barrerz, M. D., García, M. T., Zhang, Q. -A. and Álvarez-Mateos, P. (2019b). Determination of the acidity of waste cooking oils by near infrared spectroscopy. *Processes,* 7, 1–7.

Girolamo, A. D., Lippolis, V., Nordkvist, E. & Visconti, A. (2009). Rapid and non-invasive analysis of deoxynivalenol in durum and common wheat by Fourier-Transform Near Infrared (FT-NIR) spectroscopy. *Food Additives & Contaminants Part A,* 26, 907–917.

Gowen, A. A., O' Sullivan, C. & O' Donnell, C. P. (2012). Terahertz time domain spectroscopy and imaging: Emerging techniques for food process monitoring and quality control. *Trends in Food Science and Technology,* 25, 40–46.

Gómez-Mejía, E., Rosales-Conrado, N., León-González, M. E. & Madrid, Y. (2019). Citrus peels waste as a source of value-added compounds: extraction and quantification of bioactive polyphenols. *Food chemistry*, 295, 289–299.

Helland, I. S., Næs, T. & Isaksson, T. (1995). Related versions of the multiplicative scatter correction method for preprocessing spectroscopic data. *Chemometrics and Intelligent Laboratory Systems*, 29, 233–241.

Huang, H., Liu, L. & Ngadi, M. O. (2017). Assessment of intramuscular fat content of pork using NIR hyperspectral images of rib end. *Journal of Food Engineering*, 193, 29–41.

Ishiwata, N., Feng, L., Yian, N., Yoshida, M., Palihakkara, I. R., Silva, N., Tanaka, H. & Nga, N. T. (2013). Reduction of waste from beverage industry in Shizuoka prefecture. Available at http://www.iai.ga.a.u-tokyo.ac.jp/mizo/lecture/noukoku-1/group-work/2012/G2_e.pdf.

Jain, A. S.., Sushma, P. Dharmashekar, C., Beelagi, M. S., Prasad, S. K., Shivamallu, C., Prasad, A., Syed, A., Marraiki, N., & Prasad, K. S. (2020). *In silico* evaluation of flavonoids as effective antiviral agents on the spike glycoprotein of SARS-CoV-2. *Saudi Journal of Biological Sciences*, in press.

Jia, B. B., Yoon, S. -C., Zhuang, H., Wang, W. & Li, C. Y. (2017). Prediction of pH of fresh chicken breast fillets by VNIR hyperspectral imaging. *Journal of Food Engineering*, 208, 57–65.

Jo, S., Kim, S., Kim, D. Y., Kim, M.-S. & Shin, D. H. (2020). Flavonoids with inhibitory activity against SARS-CoV-23CLpro. *Journal of Enzyme Inhibition and Medicinal Chemistry*, 35, 1539–1544.

Karacaglar, N. N. Y., Bulat, T., Boyaci, I. H. & Topcu, A. (2019). Raman spectroscopy coupled with chemometric methods for the discrimination of foreign fats and oils in cream and yogurt. *Journal of Food and Drug Analysis*, 27, 101–110.

Kim, D.-S. & Lim, S. -B. (2020). Kinetic study of subcritical water extraction of flavonoids from *citrus unshiu* peel. *Separation and Purification Technology*, 250, 117259.

Lee, C. J., Wilson, L., Jordan, M. A., Nguyen, V., Tang, J. & Smiyun, G. (2010). Hesperidin suppressed proliferations of both human breast cancer and androgen-dependent prostate cancer cells. *Phytotherapy Research*, 24, S15–19.

Li, H., Wu, J. Z., Liu, C. L., Sun, X. R. & Yu, L. (2018). Study on pretreatment methods of terahertz time domain spectral image for maize seeds. *IFAC-PapersOnLine*, 51, 206–210.

Li, X. W., Geng, M. M., Peng, Y. Z., Meng, L. S. & Lu, S. M. (2020). Molecular immune pathogenesis and diagnosis of COVID-19. *Journal of Pharmaceutical Analysis*, 10, 102–108.

Liu, H. -B., Zhong, H., Karpowicz, N., Chen, Y. Q. & Zhang, X. -C. (2007). Terahertz spectroscopy and imaging for defense and security applications. *In Proceedings of the IEEE*, 95, 1514–1527.

Liu, J. (2016). Terahertz spectroscopy and chemometric tools for rapid identification of adulterated dairy product. *Optical and Quantum Electronics*, 49, 1–8.

Liu, J. J. & Li, Z. (2014). The terahertz spectrum detection of transgenic food. *Optik*, 125, 6867–6869.

Liu, W., Liu, C. H., Hu, X. H., Yang, J. B. & Zheng, L. (2016). Application of terahertz spectroscopy imaging for discrimination of transgenic rice seeds with chemometrics. *Food Chemistry*, 210, 415–421.

Maleki, S. J., Crespo, J. F. & Cabanillas, B. (2019). Anti-inflammatory effects of flavonoids. *Food Chemistry*, 299, 125124.

Nakajima, S., Shiraga, K., Suzuki, T., Kondo, N. & Ogawa, Y. (2019). Quantification of starch content in germinating mung bean seedlings by terahertz spectroscopy. *Food Chemistry*, 294, 203–208.

Nunes, K. M., Andrade, M. V. O., Almeida, M. R., Fantini, C. and Sena, M. M. (2019). Raman spectroscopy and discriminant analysis applied to the detection of frauds in bovine meat by the addition of salts and carrageenan. *Microchemical Journal*, 147, 582–589.

Ok, G., Kim, H. J., Chun, H. S. & Choi, S.-W. (2014). Foreign-body detection in dry food using continuous sub-terahertz wave imaging. *Food Control*, 42, 284–289.

Park, J. -H., Lee, M. H. & Park, E. J. (2014). Antioxidant activity of orange flesh and peel extracted with various solvents. *Preventive Nutrition and Food Science*, 19, 291–298.

Qin, J. Y., Xie, L. J. & Ying, Y. B. (2017). Rapid analysis of tetracycline hydrochloride solution by attenuated total reflection terahertz time-domain spectroscopy. *Food Chemistry*, 224, 262-269.

Roohbakhsh, A., Parhiz, H., Soltani, F., Rezaee, R., Iranshahi, M. (2015). Molecular mechanisms behind the biological effects of hesperidin and hesperetin for prevention of cancer and cardiovascular diseases. *Life Science,* 124, 64–74.

Sawalha, S. M. S., Arráez-Román, Segura-Carretero, A. & Fernández-Gutiérrez, A. (2009). Quantification of main phenolic compounds in sweet and bitter orange peel using CE-MS/MS. *Food Chemistry,* 116, 567–574.

Shen, F., Yang, D., Ying, Y., Li, B., Zheng, Y. & Jiang, T. (2012). Discrimination between Shaoxing wines and other Chinese rice wines by near-infrared spectroscopy and chemometrics. *Food Bioprocess Technology,* 5, 786–795.

Stanisic, D., Liu, L. H. B., Santos, R. V., Costa, A. F., Durán, N. & Tasic, L. (2020). New sustainable process for hesperidin isolation and anti-ageing effects of hesperidin nanocrystals. *Molecules,* 25, 4534.

Suzuki, T., Ogawa, Y. & Kondo, N. (2011). Characterization of Pesticide Residue, cis-Permethrin by Terahertz Spectroscopy. *Engineering in Agriculture, Environment and Food,* 4, 90–94.

Toledo-Guillén, A. R., Higuera-Ciapara, I., García-Navarrete, G. & Fuente, J. C. (2010). Extraction of bioactive flavonoid compounds from orange (Citrus sinensis) peel using supercritical CO_2. *Journal of Biotechnology,* 150, 314

Uchiyama, N., Kim, I. H., Kikura-Hanajiri, R., Kawahara, N., Konishi, T. & Goda, Y. (2008). HPLC separation of naringin, neohesperidin and their C-2 epimers in commercial samples and hearbal medicines.

Ueno, Y. & Ajito, K. (2008). Analytical terahertz spectroscopy. *Analytical Sciences*, 24, 185–192.

Wang, C., Zhou, R.-Y., Huang, Y.-X., Xie, L. J. & Ying, Y. B. (2019). Terahertz spectroscopic imaging with discriminant analysis for detecting foreign materials among sausages. *Food Control*, 97, 100–104.

Wang, X. -H. & Wang, J. -P. (2019). Effective extraction with deep eutectic solvents and enrichment by microporous adsorption resin of flavonoids from *Carthamus tinctorius* L. *Journal of Pharmaceutical and Biomedical Analysis*, 176, 112804.

Wu, C. R., Liu, Y., Yang, Y. Y., Zhang, P., Zhong, W., Wang, Y. L., Wang, Q. Q., Xu, Y., Li, M. X., Li, X. Z., Zheng, M. Z., Chen, L. X. and Li, H. (2020). Analysis of therapeutic targets for SARS-CoV-2 and discovery of potential drugs by computational methods. *Acta Pharmaceutica Sinica B,* 10, 766-788.

Yasui, T., Iyonaga, Y., Hsieh, Y.-D., Sakaguchi, Y., Yokoyama, S., Inaba, H., Minoshima, K., & Araki, T. (2012). Frequency-swept asynchronous-optical-sampling THz time-domain spectroscopy, *in Proceedings of the 37th International Conference on Infrared, Millimeter, and Terahertz Waves*, Wonllongong, NSW, 1-2.

Table 1 The comparison of crude and precipitation efficiencies using different extraction solvents

Extraction solvents	Crude extract efficiency (%)	Precipitate extract efficiency (%)
100% Methanol	43.20 ±8.93	0.81 ± 0.62
80% Methanol	103.76 ±9.86	0.03 ± 0.01
100% Ethanol	135.28 ± 55.64	0.16 ± 0.13
80% Ethanol	95.25 ± 18.72	0.05 ± 0.05

Table 2 Statistical parameter for predicting concentration of tablets made from standard hesperidin and naringin based on selected frequency range using PLSR with different pre-treatments.

	Terahertz range	Treatments	Calibration group		Prediction group		Cross Validation	
	0.5 – 7.0 THz		R_c^2	RMSEC (%)	R_p^2	RMSEP (%)	R_{cv}^2	RMSECV (%)
Hesperidin		Raw	0.97	3.73	0.98	3.52	0.98	3.62
		Normalization	0.93	6.19	0.89	9.05	0.90	7.74
		1st Deviation	0.98	2.89	0.99	2.97	0.99	2.85
		2nd Deviation	0.99	2.58	0.98	4.21	0.99	2.78
		MSC	0.91	7.01	0.92	7.70	0.90	7.64
		SNV	0.92	6.76	0.92	7.52	0.91	7.56
Naringin	0.5 - 7 THz	Raw	0.99	2.71	0.97	4.48	0.99	2.81
		Normalization	0.94	6.11	0.93	6.68	0.03	24.91
		1st Deviation	0.99	0.70	0.92	7.21	0.96	5.10
		2nd Deviation	0.99	1.22	0.82	10.68	0.93	6.64
		MSC	0.90	7.81	0.94	6.32	0.91	7.41
		SNV	0.91	7.59	0.94	6.17	0.92	7.23

Note: MSC: multiplicative scatter correction; SNV: standard normal variate; RMSEC: the root mean square error of calibration; RMSEP: the root mean square error of prediction; RMSECV: the root mean square error of cross validation.

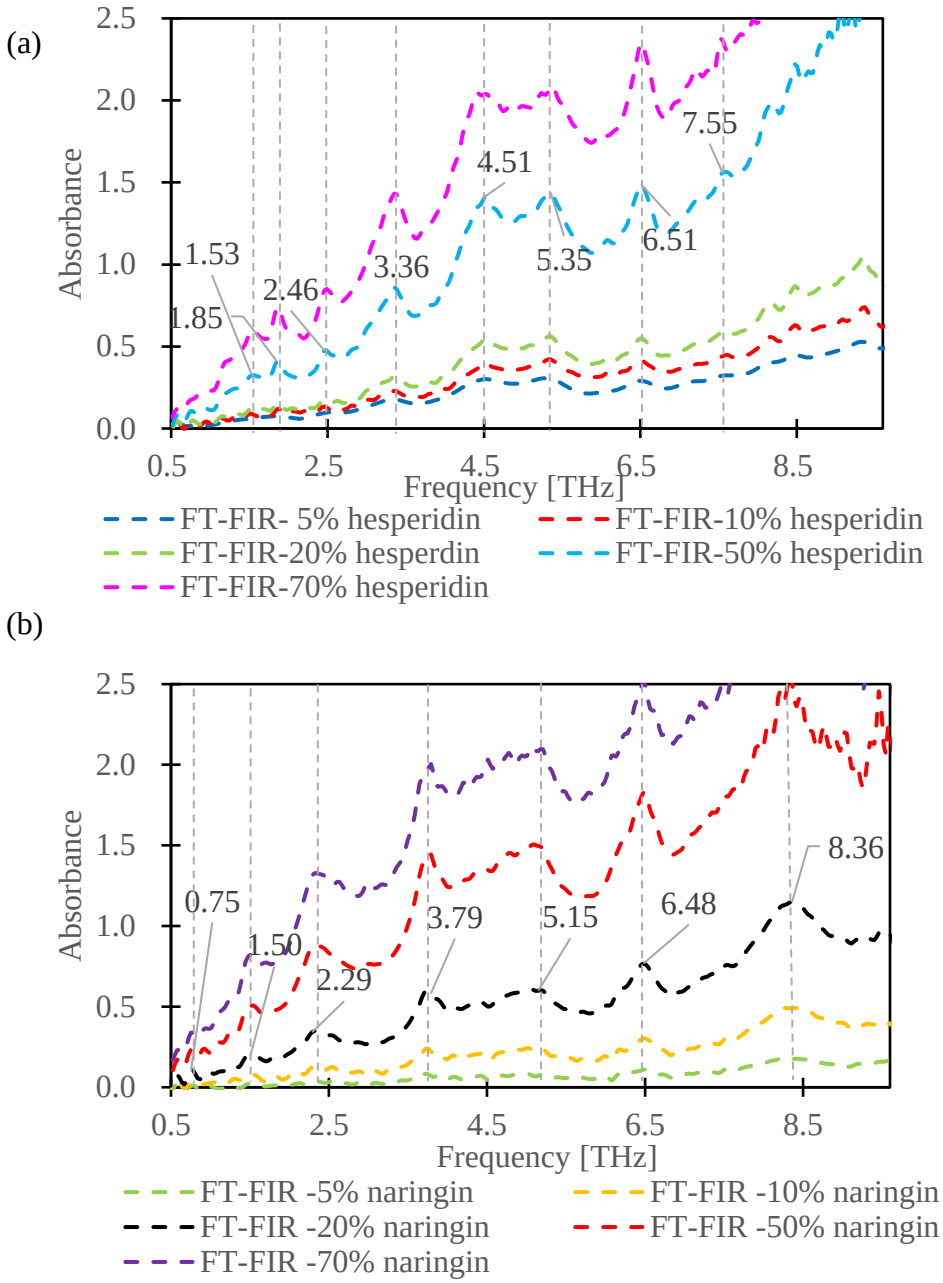

1 Figure 1. Absorbance spectra of standard hesperidin (a) and naringin (b) mixture in polyethylene that

2 measured using Fourier transform far-infrared spectrometer.

3 Note: FT-FIR: Fourier transform far-infrared spectrometer

4

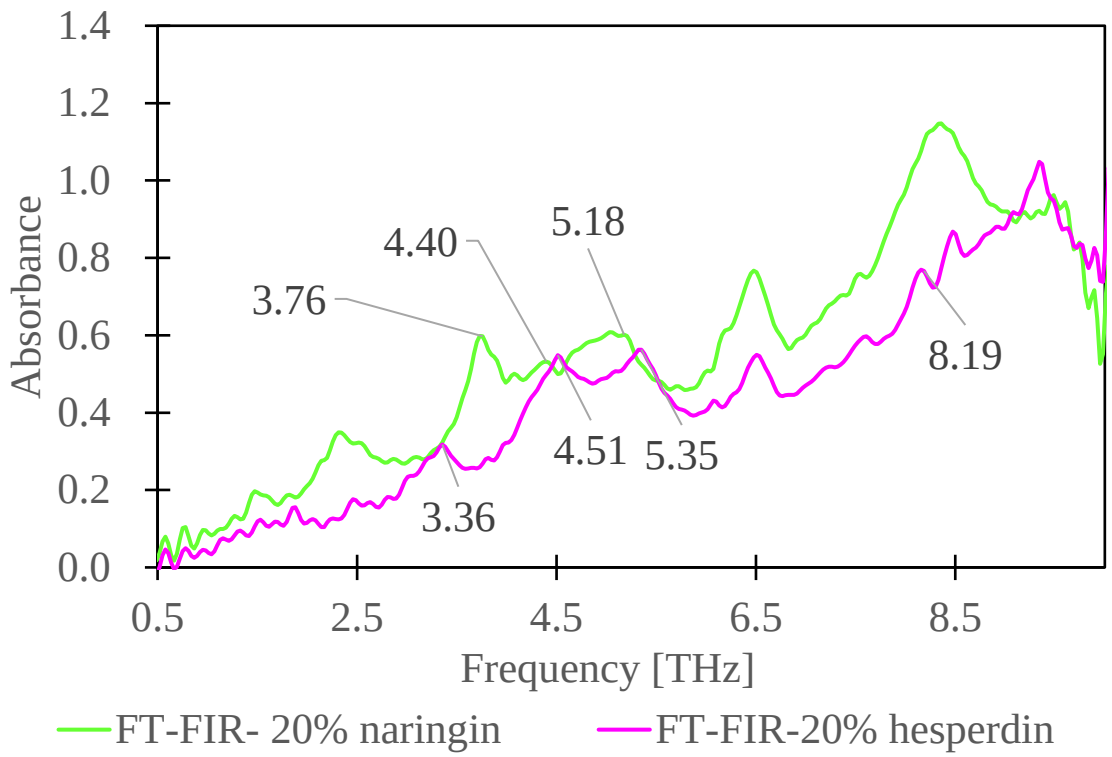

5 Figure 2. Absorbance spectra comparison of tablets made from hesperidin and naringin mixed with

6 polyethylene (concentration: 20%), being measured using Fourier transform far-infrared spectrometer.

7 Note: FT-FIR: Fourier transform far-infrared spectrometer

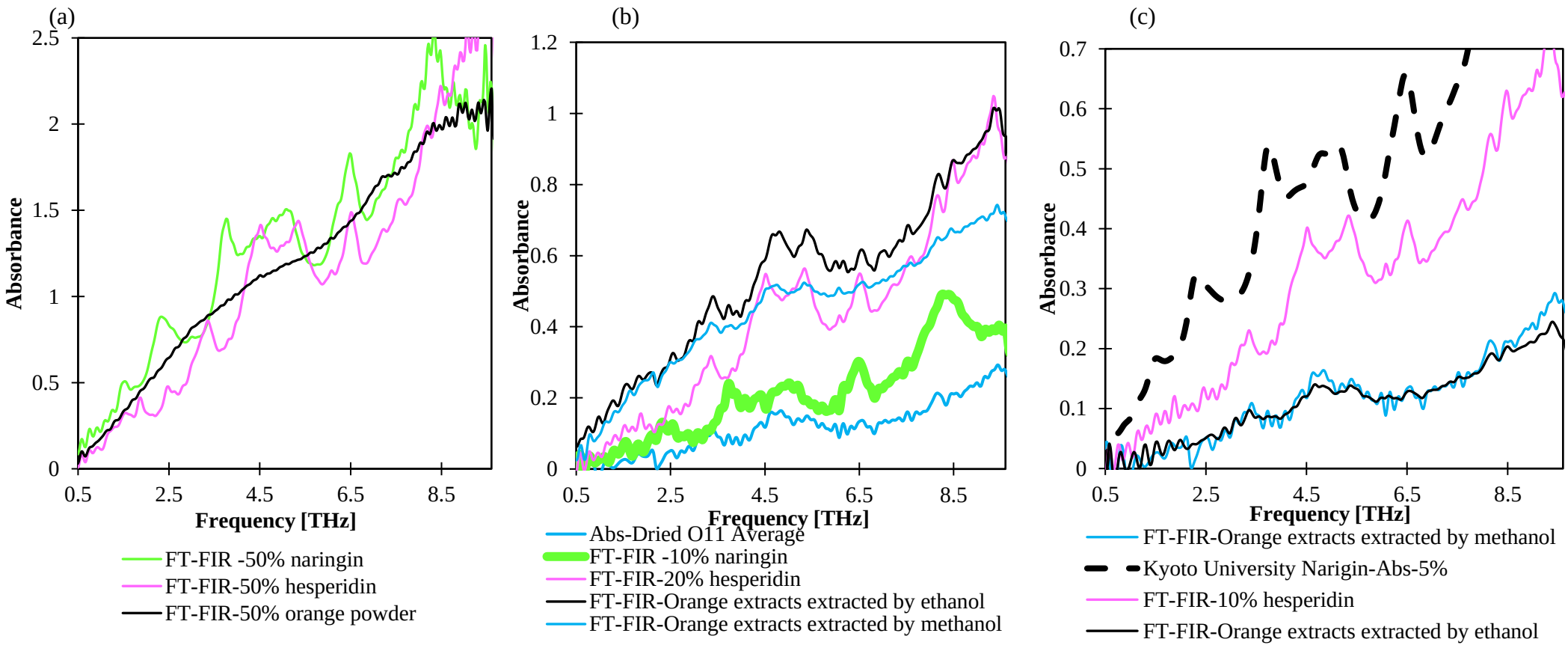

Figure3. Absorbance spectra comparison of tablets made from orange powder (a), precipitated extracts using 100% (b) and 80% (c) extraction solvents, being measured using Fourier transform far-infrared spectrometer.

Note: FT-FIR: Fourier transform far-infrared spectrometer; The percentages before the naringin, hesperidin, and orange powder mean the concentration of the tablets.